The Effect of the Welding Direction on Fatigue Crack Propagation Rate of Welded Shell Kil

By Agung Mataram

Journal of Physics: Conference Series

The Effect of the Welding Direction on Fatigue Crack Propagation Rate of Welded Shell Kiln

To cite this article: Akbar Teguh Prakoso *et al* 2019 *J. Phys.: Conf. Ser.* **1198** 042013

The Effect of the Welding Direction on Fatigue Crack Propagation Rate of Welded Shell Kiln

Akbar Teguh Prakoso, Irsyadi Yani, Agung Mataram, Gunawan, Hasan Basri[*]

Department of Mechanical Engineering, Faculty of Engineering, Universitas Sriwijaya, Indralaya 30662, Sumatera Selatan, Indonesia.

[*]E-mail: hasan_basri@unsri.ac.id

Abstract. In this paper, the fatigue crack growth rate (FCGR) properties of welded kiln shell at various positions relative to the weld has been proposed. This is achieved by combining an experimental and three-dimensional finite element model are used to demonstrate the results of fatigue crack growth rate curves in the kiln welded shell. Experimental marked crack fronts are used to determine the da/dN at local regions and provide the profile information for FE modeling. Stress Intensity Factor (SIF) at local regions is determined by FE analysis and the driving force ΔK of FCGR can be derived. Furthermore, from the mixture method, material constants of Paris law (c and m) on a welded-parts and non-welded part is measured. When crack grow across the weld-line, material constants of Paris law vary according to the effect of the welded part. In the result, the constant of Paris can be used to predict a fatigue crack growth of rotary kiln structure in finite element analysis.

Keywords: Fatigue crack growth rate, Kiln welded shell, Paris Law constants

1. Introduction

Cement rotary kiln in PT Semen Baturaja Indonesia is a large-scale weld rotary cylindrical structure of 75 m length and 4.5 m diameter. It's manufactured by welding one thin cylindrical steel plate to another, and the padded plates are directly soldered to shell on the location of supporting rollers in order to reduce the stress concentration. Rotary cement kiln operation at cycling and thermal load with variation in demand have the potential to generate fatigue loading. Complex cyclic loading conditions on kiln shell welded can promote fatigue cracks, and cracks propagate until a catastrophic fracture. Crack in welded shell kiln is often initiated at these welded joints, and the overlong circumferential cracks are prevailing at weld joints near the supporting tyre. In practice, such kiln in PT. Semen Baturaja, fatigue crack growth along the welded kiln shell may occur as shown in Figure 1.

Many companies in the industrial sector have paid a lot of attention to cope with this field observed crack, specifically the overlong circumferential cracks prevailing at weld joint in the shell kiln. Since exposure to cyclic loads is generally inevitable, fatigue crack growth (FCG) in this section is a concern. Therefore, a thorough fatigue analysis of weld shell in crack propagation stage is required in order to assess its load carrying capacity, remaining service lifetime.

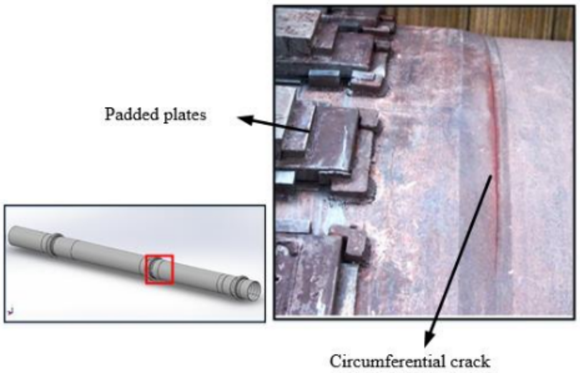

Figure 1. Crack in rotary welded shell kiln near the supporting tyre

Fatigue crack growth rate on welded structure has been investigated as outlined in a recent paper [1][2][3][4][5][6]. In this phenomenon, fatigue crack growth period is often thought to be representing almost the entire fatigue life of weldments because it believes that the fatigue crack initiation period in the welded joint is relatively short [7]. Although the fatigue crack growth analysis on welded structure has been performed, the effect of fatigue crack growth rate analysis of rotary kiln exactly in the welded shell has not been extensively studied in the past.

In this study, a mixed method combining experimental and three-dimensional (3D) finite element model to determine the fatigue crack growth rate (FCGR) curves on the kiln welded shell as indicated schematically in Figure 2. Experimental marked fronts are used to determine the da/dN at local regions and provide the profile information for FE modeling. Stress Intensity Factor (SIF) at local regions is determined by FE analysis and the driving force ΔK of FCGR can be derived. Comparison between the FCGR curves of the welded specimen determined by the mixture method has been performed. These FCGR curves are used to predict the circumferential fatigue growth behavior of welded joints on a rotary kiln structure under cyclic loading.

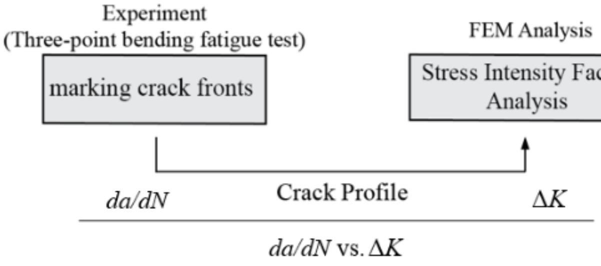

Figure 2. The experimental-FE method for fatigue crack growth rate

2. Materials and Method

2.1. Material Specimen and Preparation

Three different types of samples were adopted from a broken shell kiln in PT Semen Baturaja Indonesia as shown in Figure 3. The chemical composition (in wt.%) of material ASTM 516 Grade 70 is reported in reference [8] as shown in Table 1. The samples contain circumferential and longitudinal weld by double “v” groove Flux FCAW and SAW welding process. All specimens had the same general dimension of 45 mm × 15 mm × 9.21 mm.

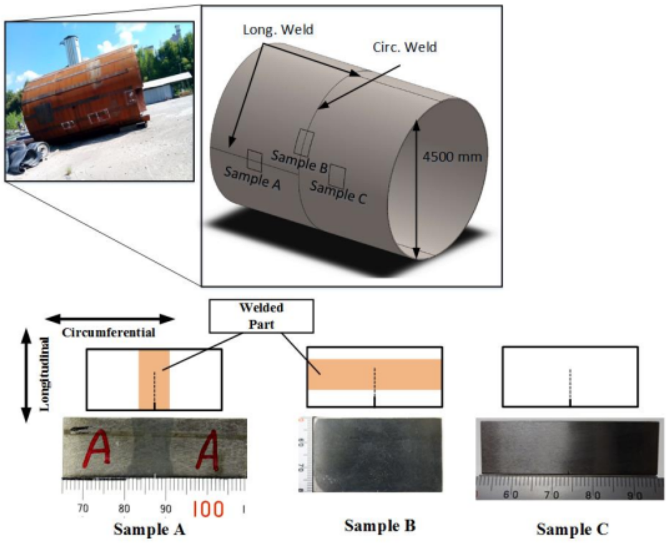

Figure 3. A photograph of a section of welded shell kiln for analysis with a different direction of welding joint (sample A: longitudinal welded direction; Sample B: circumferential welded direction; Sample C: non-welded part)

Table 1. The main chemical composition of tested material [8].

Composition	Content (wt.%)
Fe (iron)	Base Element (> 98)
C (Carbon)	0.27
Mn (Manganese)	0.79 - 1.3
S (Sulphur)	0.025
S (Silicon)	0.025

2.2. *Fatigue Crack Growth Rate and Measurement*

Fatigue crack growth testing was performed at room temperature, 293K, on MTS servo-hydraulic test machine (MTS 810) in accordance with ASTM E647-08. All specimens were tested under three-point bending. The load ratio (the ratio of the maximum to the minimum load in each loading cycle) was set R =0.1. The maximum load was set 12kN. The loading-unloading frequency was set to 5 Hz in all tests. A fatigue crack growth test was conducted on a single edge notched bend (SENB) specimens with a dimension of 45 mm × 15 mm × 9.21 mm (see Figure 4).

The notch with the depth of 1 mm was machined by electrostatic discharge machining in the middle of the specimen, which acted as a stress concentrator to initiate the crack during the test. In addition, the mechanical properties of ASTM 516 Grade 70 include Young's modulus $E = 200$ GPa, yield strength $\sigma_y = 260\ MPa$, density $\rho = 7850$ kg/m^3 and Poisson's ratio $\upsilon = 0.29$ [9]. In order measuring the fatigue crack growth parameter, the first and the most popular expression characterizing material properties from the point of view of the material resistance to fatigue crack growth in the Paris equation.

$$\frac{da}{dN} = C(\Delta K)^m$$

When da/dN is the fatigue crack growth rate, ΔK is the stress intensity factor range at the deepest and surface points respectively. C and m are material constant and should be determined by the experimental test.

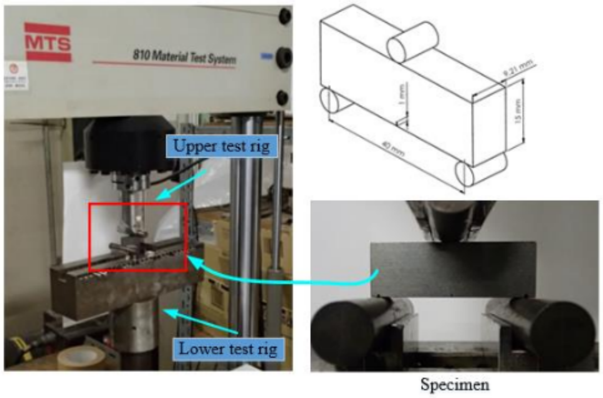

Figure 4. Schematic of a Single Edge Notch Bending test

In order to make the crack front visible on the fracture surface, a changing stress ratio method is used to generate beach marks as proposed in reference [10][11]. The fatigue load was reduced to one-half after some load cycles to produce beach marks. The illustration of marking load as shown in Figure 5.

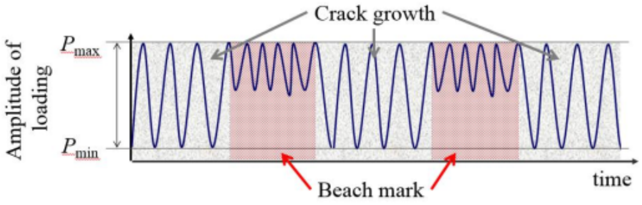

Figure 5. Illustration of the load condition of beach marks marking method

Values and ΔK were performed using FAST software by repeatedly loading the geometry, recording stress intensity factor K_I at the rack tip, advancing the crack and then unloading. The FAST software calculated the stress intensity factors for all nodes of the crack front on the basis of the FE-Solution as proposed in previous method [12]. Those stress intensity factors serve for calculation of the new crack front coordinates of the following simulation step as well as for the determination of the number of loading cycles, that are necessary for a particular crack increment. The automatic crack growth simulation is continued until *e.g.* the fracture toughness of the material is exceeded. The geometry of virtual model is same as an experimental specimen. The boundary condition as shown in Figure 6.

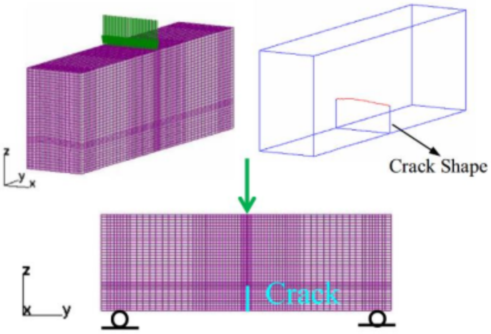

Figure 6. The boundary condition of the kiln shell specimen with a semi-elliptical surface crack

3. Results and Discussion

Fatigue crack growth behavior after the test is shown in Figure 7. Beach marks are clearly observed and crack growth rate is measured easily. Beach marks on the fracture surface generated by reducing the fatigue load have been successfully applied to welded shell kiln material. Figure 7 shows the fracture surface with beach marks obtained by means of the proposed method. The clear appearance of the crack fronts on the fracture surface indicates its applicability. The crack fronts can be measured directly from the fracture surface.

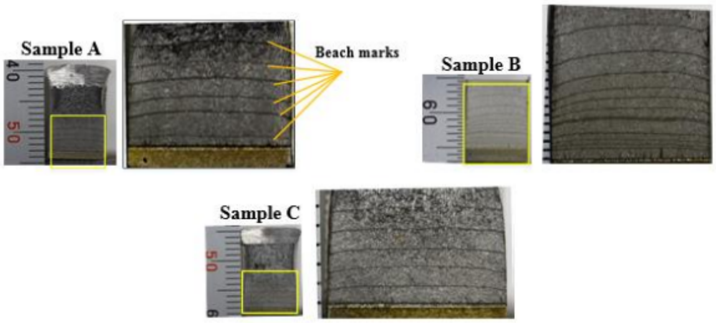

Figure 7. Fracture surface with beach marks obtained by experimental testing

The relationships between the fatigue crack growth rates (da/dN) of all materials tested under SENB and the stress-intensity factor range (ΔK) (fatigue crack growth rate) is shown in Figure 8. Figure 8 shows the effect of the weld of the specimen on the fatigue-crack growth rates of the specimens from (weld and non-weldment) and the threshold stress-intensity factor range ΔK_{th} of all specimens not significantly change. Therefore, crack growth rate (da/dN) of sample A and C slightly higher than sample B. The results showed that the welding direction had an effect on the fatigue crack growth rate. On the other hand, there was no difference in the threshold stress-intensity factor range ΔK_{th} between sample *A*, *B* and *C*.

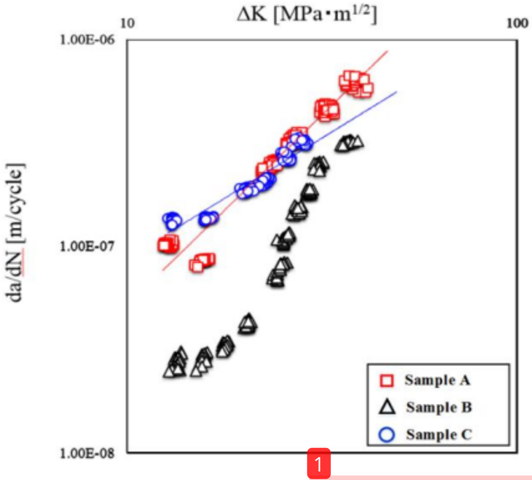

Figure 8. Effects of weldment and non-weldment on fatigue crack growth measured by fatigue crack growth testing

From the experimental testing, the material constants *C* and *m* of each sample determined by the Paris equation (Region II) in the fatigue-crack growth test are summarized in Table 2.

Table 2. Comparison of *m* and *c* obtained by fatigue crack growth test (SENB)

Specimen	C	m
A	7.383×10^{-10}	1.8
B	4.99×10^{-12}	3.2
C	5.951×10^{-9}	1.2

4. Conclusions

Fatigue crack growth rate (FCGR) tests were performed on specimens removed from welded shell kiln. An analysis procedure is presented for predicting FCG rate in welded longitudinal and circumferential butt joint on shell kiln have been investigated. Comparisons are made with measured crack growth rates in a welded longitudinal, circumferential and non-weldment under constant amplitude load. Material constants of Paris law on the specimen are measured. When crack grows across the weld-line, material constants of Paris law vary according to the effect of the welded part. From the experimental result, the constant of Paris can be used to predict a fatigue crack growth of rotary kiln structure in finite element analysis.

5. References

[1] Y. P. Shen, G. F. Bin, and S. L. Wang, “Fatigue Propagation Lifetime Prediction of Rotary Kiln Weld Shell,” *Appl. Mech. Mater.*, vol. 34–35, pp. 1724–1729, 2010.

[2] B. Baik, K. Yamada, and T. Ishikawa, “Fatigue crack propagation analysis for welded joint subjected to bending,” *Int. J. Fatigue*, vol. 33, no. 5, pp. 746–758, 2011.

[3] J. Shi *et al.*, “Fretting fatigue fracture of the supporting shaft in a rotary kiln,” *Eng. Fail. Anal.*, vol. 82, pp. 474–480, 2017.

[4] D. Radu, T. F. Galatanu, and D. Taus, “Fatigue Assessment and Behavior of a Shell Steel Element Welded Joint,” in *Procedia Engineering*, 2017, vol. 181, pp. 159–166.

[5] G. Liu, Y. Huang, M. Gao, and Y. Li, “Comparison of Shell and Solid Elements for Hot Spot Stress Analysis of Complex Welded Joints,” *Isope*, vol. 8, pp. 68–74, 2011.

[6] M. D. Chapetti and L. F. Jaureguizahar, “Fatigue behavior prediction of welded joints by using an integrated fracture mechanics approach,” *Int. J. Fatigue*, vol. 43, pp. 43–53, 2012.

[7] A. Chattopadhyay, G. Glinka, M. El-Zein, J. Qian, and R. Formas, “Stress Analysis and Fatigue of welded structures,” *Weld. World*, vol. 55, no. 7–8, pp. 2–21, 2011.

[8] C. Prieto, C. Barreneche, M. Martínez, L. F. Cabeza, and A. I. Fernández, “Thermomechanical testing under operating conditions of A516Gr70 used for CSP storage tanks,” *Sol. Energy Mater. Sol. Cells*, vol. 174, pp. 509–514, 2018.

[9] H. Basri, I. Yani, and A. Teguh Prakoso, “Vibration analysis of rotary cement kiln using finite element method,” in *MATEC Web of Conferences*, 2017, vol. 101.

[10] R. Branco, F. V. Antunes, J. D. Costa, F. P. Yang, and Z. B. Kuang, “Determination of the Paris law constants in round bars from beach marks on fracture surfaces,” *Eng. Fract. Mech.*, vol. 96, pp. 96–106, 2012.

[11] I. S. Putra and J. Schijve, “Crack Opening Stress Measurements of Surface Cracks in 7075-T6 Aluminium Alloy Plate Specimen Through Electron Fractography,” *Fatigue Fract. Eng. Mater. Struct.*, vol. 15, no. 4, pp. 323–338, 1992.

[12] M. S. Shaari, M. R. M. Akramin, A. K. Ariffin, S. Abdullah, and M. Kikuchi, “Fatigue crack growth behaviour of semi-elliptical surface cracks for an API 5L X65 gas pipeline under tension,” *IOP Conf. Ser. Mater. Sci. Eng.*, vol. 308, no. 1, pp. 0–6, 2018.

The Effect of the Welding Direction on Fatigue Crack Propagation Rate of Welded Shell Kil

ORIGINALITY REPORT

15%

SIMILARITY INDEX

PRIMARY SOURCES

1	mdpi.com Internet	71 words — 3%
2	mme.uwaterloo.ca Internet	70 words — 3%
3	karyailmiah.uho.ac.id Internet	49 words — 2%
4	mammp-journal.springeropen.com Internet	48 words — 2%
5	Joseph A. Ronevich, Christopher R. D'Elia, Michael R. Hill. "Fatigue crack growth rates of X100 steel welds in high pressure hydrogen gas considering residual stress effects", Engineering Fracture Mechanics, 2018 Crossref	43 words — 2%
6	H. Hosseini-Toudeshky. "Mixed-mode 3-D crack propagation of repaired thin aluminum panels using single-side composite patches", International Journal of Fracture, 10/2008 Crossref	31 words — 2%

EXCLUDE QUOTES	OFF	EXCLUDE SOURCES	< 2%
EXCLUDE BIBLIOGRAPHY	ON	EXCLUDE MATCHES	OFF